Phototransformation of anthraquinone-2-sulphonate in aqueous solution

Phototransformation of anthraquinone-2-sulphonate in aqueous solution

Andrea Bedini,[a] Elisa De Laurentiis,[a] Babita Sur,[a,b] Valter Maurino,[a] Claudio Minero,[a] Marcello Brigante,*[c,d] Gilles Mailhot[c,d] and Davide Vione*[a,e]

Anthraquinone-2-sulphonate (AQ2S) is a triplet sensitiser that has recently been used to model the photoreactivity of chromophoric dissolved organic matter (CDOM). We show that the photolysis quantum yield of AQ2S under UVA irradiation varies from $(3.4\pm0.2)\cdot10^{-3}$ at μM AQ2S levels to $(1.8\pm0.1)\cdot10^{-2}$ at 3 mM AQ2S (μ±σ). This trend is consistent with a combination of direct phototransformation and transformation sensitised by a photogenerated reactive species. In both cases a transient water adduct of AQ2S would be involved. Depending on the initial quinone concentration, the adduct could undergo transformation, give back ground-state AQ2S or react with it. The prevalence of the latter process at high AQ2S concentration would account for the increased values of the photolysis quantum yield. When using AQ2S as a triplet sensitiser, one should not exceed an initial concentration of 0.1 mM. Under the latter conditions the sensitised process is negligible compared to the direct photolysis, providing a simpler system to be studied, and the photolysis quantum yield is independent of the initial AQ2S concentration. This paper also shows, by adoption of density functional theory calculations, that the triplet state of AQ2S has most of the spin density localised on C=O, in analogy with other photoactive quinones, which accounts for the oxidising character of the triplet state that tends to be reduced to a semiquinone radical.

Introduction

Sunlight can induce important transformation reactions of organic and inorganic compounds in the environment, some of which take place by direct photolysis. The indirect or sensitised reactions can also be very important, especially for the transformation of substrates that do not absorb sunlight or that undergo limited or negligible direct photolysis.[1-3]

Photosensitised reactions are the consequence of radiation absorption by photoactive compounds and proceed *via* the formation of transient species. Examples of such transients are reactive radicals (*e.g.* $^{\bullet}OH$ and $CO_3^{-\bullet}$), singlet oxygen and excited triplet states.[4-6] The triplet states of some organic compounds, such as aromatic carbonyls and quinones, are able to sensitise the transformation of organic and inorganic molecules in aqueous solution by transfer of energy, electrons or hydrogen atoms.[7-9] A major issue is that the naturally occurring photosensitisers are still poorly characterised and their structures have only partially been elucidated. For this reason, it is very common to use single photoactive compounds as proxies to simulate the reactivity of natural photosensitisers that occur in surface waters (as components of the chromophoric dissolved organic matter, CDOM), in soil and in airborne particles. Aromatic carbonyls and quinones have been very often used as proxies because of their likely structural similarity with the naturally occurring photoactive compounds.[10,11]

We have recently proposed the use of anthraquinone-2-sulphonate (AQ2S) for the quantification of the reaction rate constants between organic pollutants and excited triplet states.[12-14] The study of such a reactivity is very important for the modelling and the assessment of pollutant transformation photosensitised by CDOM.[2,5,10,13] The use of AQ2S in laboratory studies offers various advantages: its triplet state does not produce either $^{\bullet}OH$ or $^1O_2$, thereby avoiding major interferences; the quantum yield of triplet formation is known and the molecule is easily studied by laser flash photolysis, which provides useful input data for a quantitative assessment of the reaction kinetics.[15,16] A potential drawback of AQ2S is that its triplet state produces two additional transients, of which one is rather unreactive (with the partial exception of reaction with nitrite)[12] while the other shows some reactivity.[15,16] It has been shown that the triplet state is considerably more reactive than the other transients toward Fe^{2+}, N_3^-, nitrite, furfuryl alcohol, benzene and nitrobenzene in circumneutral solution.[12,16] An important issue is that the scavenging of triplet AQ2S by these compounds would inhibit the formation of additional transients and decrease the importance of the reactions they are involved into. A key exception to the above framework is represented by ground-state AQ2S, which is unreactive toward triplet AQ2S but reacts with one of the transients.[15,16]

A proper use of AQ2S as model photosensitiser requires a rationale for the choice of the reaction conditions (*e.g.* the initial AQ2S concentration in kinetic competition studies). Important indications can be obtained by characterising the AQ2S triplet state and related species with flash photolysis techniques and steady irradiation. The present paper is aimed at providing the missing pieces of information to that purpose. The full comprehension of the reaction kinetics of light-excited AQ2S is in fact very important for the interpretation of experimental data of photosensitised transformation. Moreover, to our knowledge no computational study is available for the characterisation of the AQ2S triplet state (AQ2S T_1). To fill the gap, this work uses quantum chemistry calculations to support and widen the experimental understanding of AQ2S photochemistry.

Experimental

Reagents and materials

Antraquinone-2-sulfonic acid, sodium salt (purity grade 97%), NaOH (99%) and H_3PO_4 (85%) were purchased from Aldrich,

tetrabutylammonium bromide (99%) from Fluka, 2-propanol (gradient grade) from VWR Int., methanol (gradient grade) from Carlo Erba (Milano, Italy). All reagents were used as received, without further purification. Water used was of Milli-Q quality.

Irradiation experiments

Irradiation was carried out in Pyrex glass cells (4.0 cm diameter, 2.3 cm height), containing 5 mL of magnetically stirred solution. The adopted radiation source was a Philips TLK 05 UVA lamp, with emission maximum at 365 nm. Lamp irradiance reached the cells mainly from the top. The incident photon flux in solution, actinometrically determined with the ferrioxalate method,[17,18] was $2.1 \cdot 10^{-5}$ Einstein L^{-1} s^{-1}. The incident UV irradiance (290-400 nm) on top of the solutions was 28±2 W m^{-2}, measured with a CO.FO.ME.GRA. (Milan, Italy) power meter.

The emission spectrum of the lamp was measured with an Ocean Optics SD 2000 CCD spectrophotometer (calibrated with an Ocean Optics DH-2000-CAL source). The absorption spectrum (molar absorption coefficient) of AQ2S was taken with a Varian Cary 100 Scan UV-Vis spectrophotometer. Addition of 2-propanol at concentration values up to 1 M (*vide infra*) did not modify the AQ2S absorption spectrum. Lamp and AQ2S spectra are reported in the Electronic Supplementary Information (hereafter ESI), Figure ESI-1.

After irradiation, the solutions were analysed by High Performance Liquid Chromatography coupled with UV detection (HPLC-UV), adopting a Merck-Hitachi chromatograph equipped with autosampler (model AS2000), two pumps (model L6000 and L6200) for high-pressure gradients and a UV detector (model L4200). The column used was a RP-C18 LichroCART (Merck, length 125 mm, diameter 4 mm), packed with LiChrospher 100 RP-18 (5 μm diameter). Elution was carried out with a 40:60 mixture of methanol and TBA/H_3PO_4 in water (5 mM TBA = tetrabutylammonium bromide, pH 2.8), at a flow rate of 1.0 mL min^{-1}. Under these conditions the column dead time was 0.90 min and the AQ2S retention time was 12.4 min. The injection volume was varied in the range of 10-100 μL and detection was carried out at 260 or 330 nm, depending on the initial concentration of AQ2S.

Monitoring of AQ2S hydroxyderivatives

To detect AQ2S hydroxyderivatives (α and β), solutions after irradiation were adjusted to pH 12 with NaOH to have the target compounds in their deprotonated form. Absorbance was measured at 475 and 491 nm with the Varian Cary 100 Scan UV-Vis spectrophotometer. Deprotonated α-hydroxyAQ2S absorbs radiation at 491 nm ($\varepsilon = 5.65 \cdot 10^3$ M^{-1} cm^{-1}), while deprotonated β-hydroxyAQ2S absorbs significantly at both 475 nm ($\varepsilon = 3.60 \cdot 10^3$ M^{-1} cm^{-1}) and 491 nm ($\varepsilon = 3.40 \cdot 10^3$ M^{-1} cm^{-1}).[19]

Radiation absorption calculations

Assume $p°(\lambda)$ as the incident spectral photon flux density in solution and $\varepsilon_{AQ2S}(\lambda)$ as the molar absorption coefficient of AQ2S (see Figure ESI-1). The figure also shows that $p°(\lambda)$ and $\varepsilon_{AQ2S}(\lambda)$ overlap in the 300-400 nm wavelength region. According to the Beer-Lambert law, the photon flux absorbed by AQ2S (P_a^{AQ2S}) can be expressed as follows:

$$P_a^{AQ2S} = \int_{\lambda} p°(\lambda)[1-10^{-\varepsilon_{AQ2S}(\lambda) b [AQ2S]}]\, d\lambda \qquad (1)$$

Equation (1) was integrated numerically by means of the FigP software package (Biosoft, UK).

Kinetic data treatment

The time evolution of AQ2S under irradiation was fitted with pseudo-first order equations of the form $[AQ2S]_t = [AQ2S]_o\, e^{-k\,t}$, where $[AQ2S]_t$ is the concentration of AQ2S at the time t, $[AQ2S]_o$ its initial concentration and *k* the pseudo-first order rate constant of AQ2S transformation. The initial transformation rate of AQ2S is $R_{AQ2S} = k\,[AQ2S]_o$. The error bounds associated to the rate data (μ±σ) were derived from the corresponding error on *k*, which in turn depends on the scattering of the experimental data points around the fit curve (intra-series variability). The reproducibility of repeated runs (inter-series variability) was around 10-15%.

Laser flash photolysis experiments

Laser flash photolysis (LFP) experiments were carried out using the third harmonic (λ_{exc} = 355 nm with an energy of ~ 45 mJ/pulse) of a Quanta Ray GCR 130-01 Nd:YAG laser system instrument, disposed on a right-angle geometry with respect to the monitoring light beam. Individual cuvette samples (3 mL volume) were used for a maximum of two consecutive laser shots. The transient absorbance at the pre-selected wavelength was monitored by a detection system consisting of a pulsed xenon lamp (150 W), monochromator and a photomultiplier (1P28). A spectrometer control unit was used for synchronising the pulsed light source and programmable shutters with the laser output. The signal from the photomultiplier was digitised by a programmable digital oscilloscope (HP54522A). A 32 bits RISC-processor kinetic spectrometer workstation was used to analyse the digitised signal.

Stock solutions of AQ2S and 2-propanol were previously prepared in Milli-Q water and were mixed to obtain the desired concentration just before each experiment. The three transient species formed upon excitation of AQ2S (here indicated as AQ2S T_1, B and C) were monitored at 380, 520 and 600 nm, respectively, as previously reported.[16] The second-order reaction rate constants with 2-propanol were determined from the regression lines of the logarithm decay constants against the alcohol concentration. All experiments were performed at ambient temperature (295 ± 2 K) in aerated solution, using Milli-Q water (pH 6.5) as the solvent.

Computational methods

Geometry optimisations were performed in the gas phase and were confirmed by analytical calculation of frequencies.[20] For each species, the gas-phase optimised structures were determined by gradient procedures [21] within the Density Functional Theory (DFT) [22] with the B3LYP hybrid functional.[23] The latter performs well with polycyclic aromatic systems and their functionalised derivatives such as the anthraquinones.[24-27] The polarised 6-311G(d,p) basis set was used in all the calculations [28,29] and the nature of the stationary points was confirmed by analytical calculation of vibrational frequencies.[18] Finally, the energy values

obtained in the gas-phase calculations were refined taking the solvent effect into account, through single-point calculations at the PCM (Polarised Continuum Method) level.[30]

The AQ2S excitation spectrum and its energy levels have been computed within the Time-Dependent Density Functional Theory (TDDFT),[31] using the hybrid functional and basis set described above. A number of 30 singlet and 30 triplet states with their related oscillator strengths were computed, starting from ground-state geometry. Only electronic transitions with an oscillator strength value (*f*) higher than 0.1 were explored. Solvent effects on the electronic structure and the excited states of AQ2S were investigated using the TDDFT theory, coupled with the PCM model in its non-equilibrium formulation for the calculation of excited state properties, ignoring the weak modifications in ground-state geometry induced by the solvent.[32]

The electronic distribution and localisation of the singlet excited states were visualised using the electron density difference maps (EDDMs).[33,34] All molecular calculations were carried out with the GAUSSIAN 03W suite of programs.[35] *GaussSum*, release version 1.05, was used for EDDM calculations and for the simulation of the UV-VIS spectrum.[36] The *GaussView* program was used to visualise optimised structures and spin distributions.

Results and discussion

Quantum mechanical calculations of the AQ2S triplet state

The gas-phase optimised structure of AQ2S in its ground state (S_0) is reported in Figure ESI-2. Preliminary calculations (both geometry optimisation and TDDFT studies) were performed on the AQ2S molecule without the sodium counter-ion. However, the results did not match with the experimental data, in particular as far as the UV-VIS spectra are concerned. Therefore, all the following calculations have taken the Na^+ counter-ion into account. The obtained structure was compared to the XRD data collected by Gamage.[37] Calculations slightly overestimated the sulphur-oxygen distances (by 0.016 Å), but all the remaining bond lengths were within 0.002 Å of the experimental ones. Therefore, the computed molecular structure can be considered as a sufficiently good model for the real one.

The lower-lying triplet (T_1) state shows some structural modifications compared to S_0: increased C=O bond length, shrinking of the central ring, lengthening of one of the S-O bonds (see ESI). Figure 1 reports the total spin density surface of AQ2S T_1 and shows two main areas where the spin density is higher. The strongest one is centred on one carbonyl group, the other on the atoms that allow the resonance of unpaired electrons on the aromatic skeleton of the molecule, including the other carbonyl group. In the former case, the high spin density is localised on the unoccupied π^* system of C=O, in analogy with the carbon monoxide molecule in its lower lying triplet state.[11] In contrast, the sulphonate group and the hydrogen atoms exhibit negligible spin density. The spin density distribution of AQ2S T_1 is very similar to that of other photoactive anthraquinones in their triplet state, while poorly reactive quinones show most of the triplet-state spin density on the aromatic skeleton.[11] It can thus be hypothesised that the C=O spin density of AQ2S T_1 is closely linked to its photoreactivity, which should involve oxidation of other molecules and reduction of AQ2S T_1 to a semiquinone radical.[38] This conclusion is supported by the length of the high-spin density C=O bond in AQ2S T_1 (see ESI), which is consistent with an incipient >C–O$^\bullet$ system that can be found in the semiquinone radical.

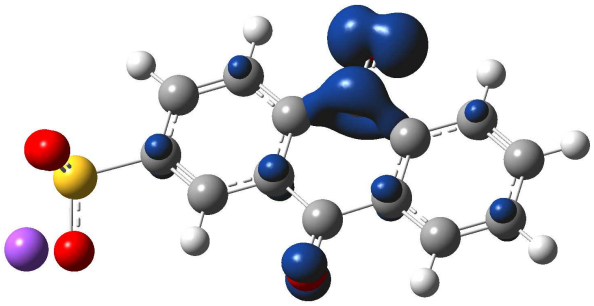

Fig. 1 Spin density surface of AQ2S in its T_1 state (isovalue = 0.02).

The TDDFT calculation was performed on the AQ2S gas-phase optimised geometry, to understand the behaviour of excited AQ2S and explore the nature and position of its energy levels. TDDFT calculations of the energy levels took the solvent effects into account within the PCM method. It can be observed that all the transitions from S_0 to the triplet states are forbidden for multiplicity rules, and that their oscillator strength is zero. Calculated absorption properties for AQ2S in aqueous solution are reported in Table ESI-1, where only transitions with an oscillator strength higher than 0.1 are considered and compared with the experimental results. Calculations are in very good agreement with experimental data, as can be seen from Figure 2 that shows a good match between experimental and simulated UV-VIS spectra for AQ2S in aqueous solution.

Figure 3 is a graphical representation of the excitation processes. It includes some EDDM (electron density difference maps), referred to singlet states reached by transitions with oscillator strength higher than 0.1, and all the energy levels of singlet and triplet states calculated in the TDDFT simulation. Each band appearing in the AQ2S UV-VIS spectrum can be assigned to a particular transition, using Braude notation.[39] Around 200 nm one finds $\pi \rightarrow \pi^*$ transitions of aromatic skeleton bonds (E bands, $S_0 \rightarrow S_{28}$, $S_0 \rightarrow S_{22}$, $S_0 \rightarrow S_{19}$). The band at 255 nm represents a $\pi \rightarrow \pi^*$ transition of the aromatic system (K band, $S_0 \rightarrow S_{10}$), characterised by strong molar absorption coefficient. The shoulder at 286 nm is supposed to be a benzenoid band (B band, $S_0 \rightarrow S_7$) whose fine structure is lost in the polar solvent. The weaker but environmentally significant band centred at 333 nm can be assigned to a $n \rightarrow \pi^*$ transition (R band, $S_0 \rightarrow S_4$).

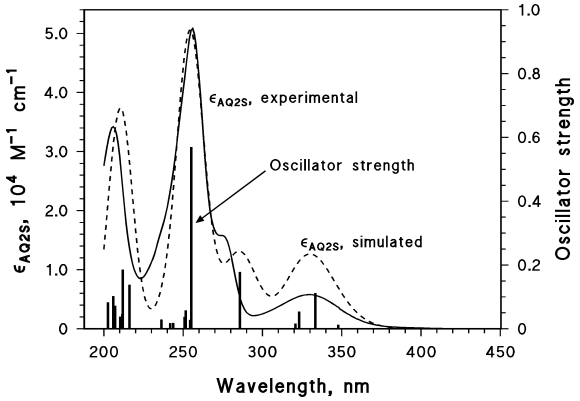

Fig. 2 Experimental (solid) and simulated (dashed) UV-Vis spectra of AQ2S in aqueous solution. The simulated curve was obtained employing *GaussSum 1.05*. The oscillator strength (right Y axis) is reported as solid bars.

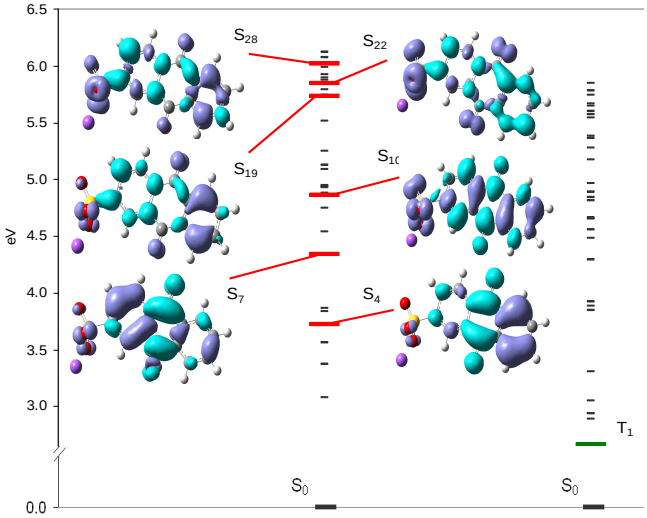

Fig. 3 Selected singlet and triplet excited states of AQ2S with their respective electron density difference maps (EDDMs), obtained using the program GaussSum 1.05 (sky blue indicates an increase in charge density, violet indicates a decrease). All major components and their relative weight were taken into consideration for each transition.

A reviewer's remark concerned the likely importance of transitions $S_0 \rightarrow S_1$ (403 nm) and $S_0 \rightarrow S_2$ (367 nm). Although weaker than $S_0 \rightarrow S_3$ or $S_0 \rightarrow S_4$, they would extend the absorbance of AQ2S right into the visible range and would produce a weak band. Such a band, which may have been experimentally detected (personal communication by anonymous reviewer), could be of interest for some applications.

Laser flash photolysis experiments

The excited triplet state of AQ2S (AQ2S T_1) is formed upon radiation absorption followed by inter-system crossing (quantum yield $\Phi_T = 0.18$ [40]). AQ2S T_1 evolves upon reaction with H_2O to form two transients, indicated in the literature as B and C.[15,16] Figure ESI-3 reports the traces of the evolution of the absorbance at 380 nm (AQ2S T_1), 520 nm (B) and 600 nm (C), clearly showing that B and C are formed while AQ2S T_1 decays. The two species B and C have variously been termed as water adducts of ground-state AQ2S [15] or water exciplexes of triplet AQ2S.[41] Triplet AQ2S forms various charge-transfer complexes (exciplexes) with oxidisable compounds, which have partial ion-couple nature and absorption spectra that are very close to that of AQ2S radical anion ($AQ2S^{-\bullet}$).[42] The latter has two clear absorption maxima at 400 and 500 nm and no absorption above 550 nm,[43] differently from B and C that have an absorption band at 600 nm and no peak at 400 nm.[16] Based on these important differences, it is hardly likely for B and C to be water exciplexes. They should rather be considered as adducts between ground-state AQ2S and water.

As far as the structure of B and C is concerned, it should be considered that laser irradiation of anthraquinone-2,6-disulphonate (AQ26DS) has yielded the same number of transients as AQ2S,[44] with absorption spectra that closely match those of AQ2S T_1, B, C, $AQ2S^{-\bullet}$ and $AQ2SH^{\bullet}$, respectively.[15,16,43,44] The structure of the AQ26DS transients that spectrally correspond to B and C has been studied by time-resolved resonance Raman spectroscopy,[45] and two water adducts have been identified. The former, corresponding to B, has the water molecule interacting with the oxygen atom of one of the two C=O groups. In the latter, corresponding to C, the water molecule interacts with one of the side aromatic rings, quite away from the sulphonate group.[45] The very good match between the absorption spectra of the intermediates of AQ26DS and AQ2S strongly suggests that B is a water adduct where H_2O hydrogen is attached to the C=O oxygen, while C is a water adduct where H_2O is attached to the side ring *via* the oxygen atom.

We have adopted 2-propanol as probe molecule to study the triplet state of AQ2S. In addition to being a well-known $^{\bullet}OH$ scavenger (which is not applicable to the present case), 2-propanol is also an effective quencher of excited states. Its use is compatible with both laser flash photolysis measurements and steady irradiation experiments. It has for instance been used to probe the reactivity of 1-nitronaphthalene as triplet sensitiser in both steady irradiation experiments and flash photolysis runs.[46] It is thus possible to use 2-propanol to test hypotheses on triplet reactivity, and to check whether they fit into a consistent framework.

In the determination of the first-order rate constants k_A, k_B and k_C, following the decay of AQ2S T_1, B and C at 380, 520 and 600 nm, respectively, a correct choice of the time intervals where to fit the flash photolysis traces can avoid the risk of biases due to spectral overlap.[15] In the case of AQ2S T_1 there is potential interference from B and C because they rise while the triplet decays, but at 380 nm the spectral interference is minimised.[16] Moreover, Figure ESI-3 shows that between 0.1 and 0.3 µs the absorbance values of B and C vary very little, which further reduces the possibility of interference in this time interval. The rise and decay of C monitored at 600 nm could be biased by B soon after the pulse. However, spectral interference by B would be minimised between 0.4 and 1.0 µs, where the absorbance of B is about constant (see Figure ESI-3). This is due to the fact that $k_B < 10^{-2}\ k_C$. AQ2S T_1 would not interfere with C, because it does not absorb significantly at 600 nm. Finally, the slow decay of B can easily be fitted over a longer time scale (> 6 µs), starting after the practically complete decay of both AQ2S T_1 and C.

Figure 4 shows the trend of the pseudo-first order rate constants for the decay of AQ2S T_1, B and C (k_A, k_B and k_C, respectively) as a function of the concentration of 2-propanol,

upon laser irradiation of 0.1 mM AQ2S. In the absence of the alcohol, from repeated laser shots one finds $k_A = (5.8\pm0.2)\cdot10^6$ s^{-1}, $k_B = (2.3\pm0.1)\cdot10^4$ s^{-1} and $k_C = (3.1\pm0.1)\cdot10^6$ s^{-1} at 380, 520 and 600 nm, respectively. From Figure 4 one gets that B is unreactive toward 2-propanol, while AQ2S T_1 and C react significantly. Indeed, the Pearson test returned significant correlation for both k_A *vs.* [2-propanol] ($p < 0.001$) and k_C *vs.* [2-propanol] ($p = 0.04$).

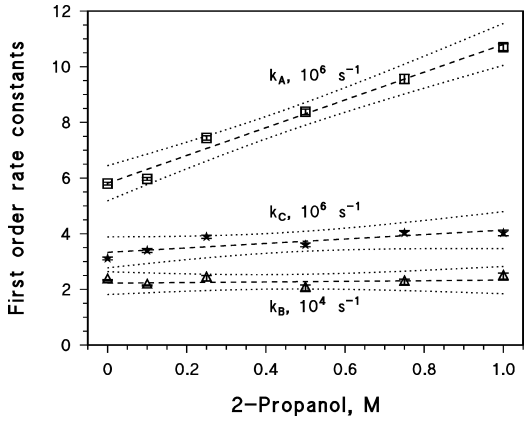

Fig. 4 Effect of 2-propanol concentration on the first-order decay constants of the species related to AQ2S T_1. The LFP experiments (355 nm, 45 mJ) were carried out in aerated solution at 295 ± 2 K and pH 6.5, in the presence of 0.1 mM AQ2S. Fit lines are dashed, 95% confidence bands of the fits are dotted. The error bars represent ±σ.

From the slopes of the lines k_A *vs.* [2-propanol] and k_C *vs.* [2-propanol] one obtains the second-order reaction rate constants of AQ2S T_1 and C with the alcohol, the respective values of which are $(4.99\pm0.30)\cdot10^6$ M^{-1} s^{-1} and $(7.99\pm2.66)\cdot10^5$ M^{-1} s^{-1}. Note the higher reactivity with 2-propanol of AQ2S T_1 compared to C, a feature that is often observed with irradiated AQ2S in the presence of organic and inorganic compounds.[12,16]

The transient species AQ2S T_1 and C are oxidising agents,[12] thus the reaction with 2-propanol would oxidise the alcohol and yield the reduced form of AQ2S. The reactions between irradiated quinones and 2-propanol proceed by hydrogen transfer,[47] thus $AQ2SH^\bullet$ would be produced. The acid-base equilibrium $AQ2SH^\bullet/AQ2S^{-\bullet}$ has $pK_a \approx 3.5$,[43] and under the conditions adopted in this study (pH 6.5) there could be deprotonation of $AQ2SH^\bullet$ to the radical anion $AQ2S^{-\bullet}$. The latter species has two absorption maxima at 400 and 500 nm.[43] Interestingly, two absorption bands at these wavelengths were detected in our experiments in the presence of 2-propanol (Figures ESI-4, ESI-5).

Figure 5 reports two transient absorption spectra obtained in the absence and in the presence of 0.4 M 2-propanol, as well as their difference. The difference spectrum has two absorption maxima at 400 and 500 nm, consistently with the spectrum of $AQ2S^{-\bullet}$.[43] The detection of $AQ2S^{-\bullet}$ under the adopted conditions suggests that deprotonation of $AQ2SH^\bullet$ would be much faster than the other decay processes of either $AQ2SH^\bullet$ or $AQ2S^{-\bullet}$.

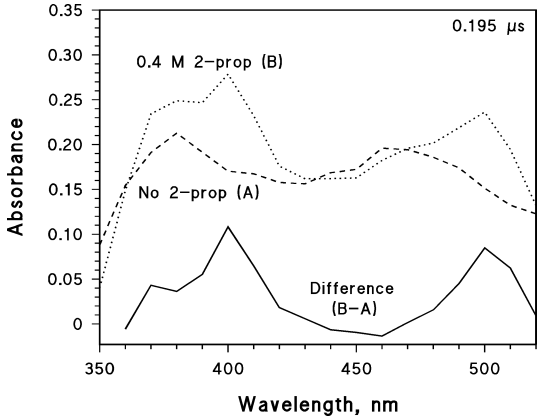

Fig. 5 Absorption spectra of the transient species formed by laser pulse irradiation of 0.1 mM AQ2S, 0.195 µs after the pulse (355 nm, 45 mJ), in the absence (A) and in the presence (B) of 0.4 M 2-propanol. The difference between the two spectra (B-A) is also reported. The experiments were carried out in aerated solution at 295 ± 2 K and pH 6.5.

Photolysis quantum yield of AQ2S as a function of its concentration, under steady irradiation conditions

The transformation of AQ2S upon UVA irradiation was studied in the concentration range of 1 µM – 3 mM, at pH 6 in aerated solution. Under the adopted conditions, AQ2S followed a pseudo-first order decay with a half-life time in the range of 100-170 min. The photolysis quantum yield was calculated as $\Phi_{AQ2S} = R_{AQ2S}\ P_{a,AQ2S}^{-1}$, where R_{AQ2S} is the initial transformation rate of AQ2S (disappearance of the substrate) and $P_{a,AQ2S}$ is its initial absorbed photon flux. The trend of Φ_{AQ2S} *vs.* the initial AQ2S concentration is reported in Figure 6.

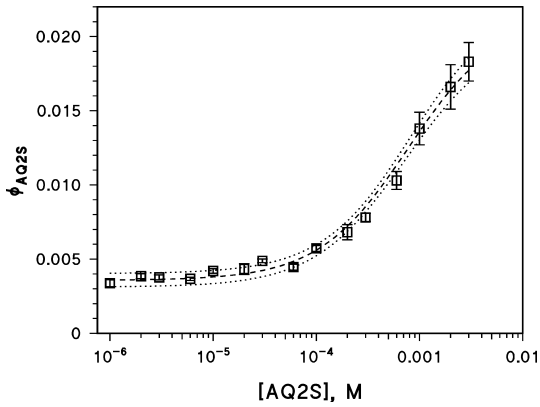

Fig. 6 Multi-wavelength photolysis quantum yield of AQ2S as a function of its initial concentration, under UVA irradiation at pH 6. The dashed curve is the data fit with equation (2), while the 95% confidence bands are dotted. Note the exponential scale of the X-axis.

One can see that Φ_{AQ2S} is almost independent of AQ2S for concentration values below 0.1 mM, and that it increases with increasing AQ2S for higher values. This trend is consistent with a significant reaction between excited and ground-state AQ2S at high concentration.[48] Literature data clearly suggest that C is the only excited AQ2S species that is able to react with ground-state AQ2S.[15,16]

Based on the literature and on our laser flash photolysis results, a reactivity scenario can be depicted for the system under study.

Radiation absorption by ground-state AQ2S (AQ2S S_0) followed by inter-system crossing gives AQ2S T_1, which reacts with water to yield B and C. Reaction of AQ2S T_1 with water is faster than either reaction with O_2 or internal conversion to the ground state.[15] B would be slowly converted back to AQ2S S_0. C could give back AQ2S S_0, undergo other transformation processes or react with AQ2S S_0.[15,16] In the latter reaction, C would be reduced and AQ2S S_0 oxidised.[16,38] The reduced species $AQ2S_{red}$ (most likely $AQ2S^{-\bullet}$ under the adopted pH 6) would react with dissolved O_2 to yield back AQ2S S_0 plus $O_2^{-\bullet}$.[15,38] The above pathways are depicted in Scheme 1a.

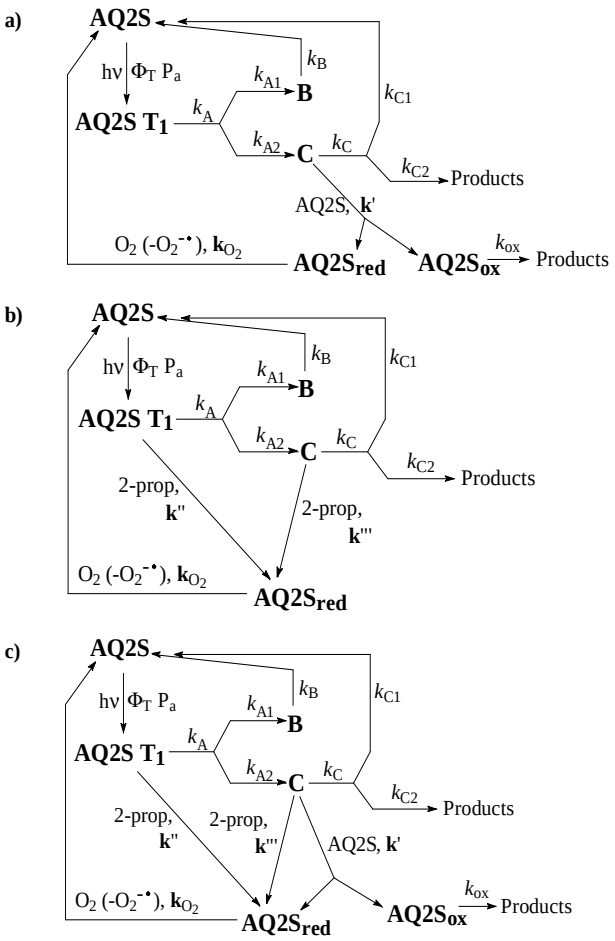

Scheme 1. Proposed reaction schemes of AQ2S alone **(a)**, of AQ2S + 2-propanol at low AQ2S **(b)** and of AQ2S + 2-propanol at high AQ2S **(c)**. From the schemes (a), (b) and (c), upon application of the steady-state approximation to AQ2S T_1, B, C and $AQ2S_{red}$, one obtains equations (2), (3) and (4), respectively. In the scheme, the first-order rate constants are in italic, the second-order ones are in bold. 2-prop = 2-propanol.

Note that AQ2S T_1 is formed with quantum yield $\Phi_T = 0.18$.[40] The quantum yields for the formation of B and C are $\Phi_B = \Phi_T\, k_{A1}\, k_A^{-1} = 0.16$ and $\Phi_C = \Phi_T\, k_{A2}\, k_A^{-1} = 0.02$.[15,16,40] Figure 6 shows that the quantum yield Φ_{AQ2S} tends to 0.02 at high AQ2S concentration, thus it is $\lim_{(high AQ2S)} \Phi_{AQ2S} \approx \Phi_C$. This behaviour is in very good agreement with the processes shown in Scheme 1a, because at sufficiently high AQ2S the whole of C would be scavenged by ground-state AQ2S.

In this context, to explain the Φ_{AQ2S} trend reported in Figure 6 it is essential to assume that C is able to give back AQ2S at some extent (with rate constant k_{C1}, see Scheme 1), in agreement with literature suggestions.[15] From the processes depicted in Scheme 1a and by applying the steady-state approximation to the transients AQ2S T_1, B, C and $AQ2S_{red}$, one gets the following expression for Φ_{AQ2S}:

$$\Phi_{AQ2S} = \frac{k_{A2}}{k_A} \cdot \Phi_T \cdot \frac{k_{C2} + k'[AQ2S]}{k_C + k'[AQ2S]} \qquad (2)$$

Assuming $k_A = 5.8 \cdot 10^6$ s^{-1} and $k_C = 3.1 \cdot 10^6$ s^{-1} as per our laser flash photolysis results and $\Phi_T = 0.18$,[40] the fit of the Figure 6 data with equation (2) yielded $k_{A2} = (6.9 \pm 0.1) \cdot 10^5$ s^{-1}, $k_{C2} = (5.2 \pm 0.3) \cdot 10^5$ s^{-1} and $k' = (4 \pm 1) \cdot 10^9$ M^{-1} s^{-1}. The value of k_{A2} obtained by numerical fit is in excellent agreement with literature reports,[15] while no previous measurement of k_{C2} could be found in the literature. The fact that $k_{C2}\, k_C^{-1} = 0.17 \pm 0.01$ implies that over 80% C would evolve back into AQ2S S_0 at low AQ2S concentration. The reaction between C and AQ2S S_0 at high concentration would enhance the quantum yield of AQ2S photolysis. As far as k' is concerned, our result compares very well with recent findings based on laser flash photolysis measurements.[16]

Formation of AQ2S hydroxyderivatives

It has long been known that α- and β-hydroxyAQ2S are formed upon AQ2S irradiation,[19] and more recent studies could only confirm that the hydroxyderivatives are the only important AQ2S phototransformation intermediates in aqueous solution.[38] Scheme 1a suggests that AQ2S derivatives could be formed by further evolution of both C and $AQ2S_{ox}$. The process involving C would likely prevail at low AQ2S, that involving $AQ2S_{ox}$ at high AQ2S. Considering that C would be a water adduct of AQ2S where the water molecule interacts with the lateral ring, the formation of AQ2S hydroxyderivatives upon transformation of C is quite reasonable. Also reasonable is the formation of hydroxyderivatives upon reaction between $AQ2S_{ox}$ and water. Figure ESI-6 reports the time trend of the absorbance at 475 and 491 nm of AQ2S solutions (initial concentration 10 µM and 2 mM, respectively), adjusted after irradiation to pH 12 with NaOH. At these wavelength values, AQ2S does not absorb radiation but the deprotonated hydroxyderivatives do.[19]

Irradiation of 10 µM AQ2S gave practically identical absorbance values at both wavelengths, while in the case of 2 mM AQ2S the absorbance at 475 nm was 10-20% higher than that at 491 nm. This means that a higher fraction of β-hydroxyAQ2S compared to α-hydroxyAQ2S was formed with 2 mM AQ2S than with 10 µM AQ2S. Such a small but detectable difference is compatible with the occurrence of two different AQ2S transformation processes, as hypothesised in Scheme 1a: evolution of the ring water-adduct C into more stable compounds at low AQ2S, and transformation of $AQ2S_{ox}$ at high AQ2S.

Effect of 2-propanol on AQ2S phototransformation

Figure 7 reports the trends of R_{AQ2S} as a function of the concentration of 2-propanol, for 20 µM (8a) and 3 mM (8b) initial AQ2S. It can be seen that in both cases, the addition of 2-propanol decreases the AQ2S transformation rate.

At 20 µM AQ2S, the substrate concentration is too low for the reaction between C and ground-state AQ2S to be significant. Therefore, C would either give back AQ2S (k_{C1}) or be transformed (k_{C2}). The laser flash photolysis results (Figure 4) suggest that 2-propanol would scavenge both AQ2S T_1 and C, with respective rate constants k'' ≅ $5.0\cdot10^6$ M^{-1} s^{-1} and k''' ≅ $8.0\cdot10^5$ M^{-1} s^{-1}. It is also suggested that AQ2S T_1 and C oxidise 2-propanol and undergo reduction to $AQ2S^{-\bullet}$ (Figure 5). To further support this assumption, we detected acetone (a typical oxidation by-product of 2-propanol [46]) upon irradiation of AQ2S and 2-propanol (data not shown).

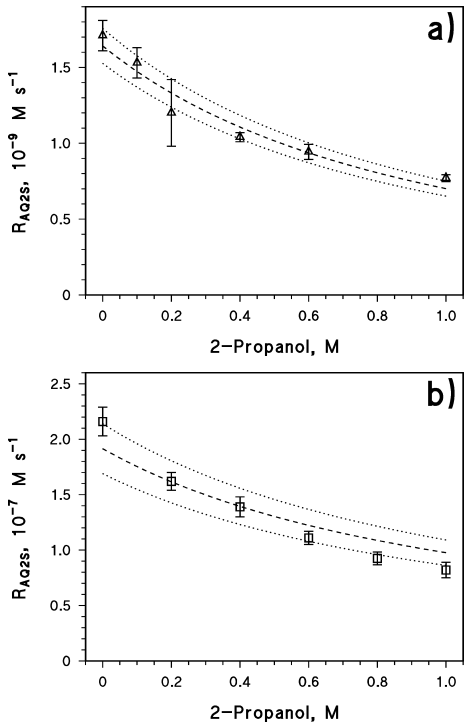

Fig. 7 **a)** Effect of the initial concentration of 2-propanol on the phototransformation rate of 20 µM AQ2S. **b)** Effect of the initial concentration of 2-propanol on the phototransformation rate of 3 mM AQ2S. UVA irradiation and pH 6 in both cases.
The dashed curves are the fit of the experimental data, with equation (3) and (4) for Figure 7a and 7b, respectively. The dotted curves are the 95% confidence bands of the fit.

With 20 µM AQ2S and 2-propanol the kinetic system reported in Scheme 1b applies, which upon application of the steady-state approximation to AQ2S T_1, B, C, and $AQ2S_{red}$ yields the following equation for R_{AQ2S} (2-Pr = 2-Propanol):

$$R_{AQ2S} = \Phi_T P_a \cdot \frac{k_{A2}\, k_{C2}}{(k_A + k''[2-\mathrm{Pr}])\,(k_C + k'''[2-\mathrm{Pr}])} \quad (3)$$

The fit of the experimental data with equation (3), assuming Φ_T = 0.18,[40] $k_A = 5.8\cdot10^6$ s^{-1}, $k_C = 3.1\cdot10^6$ s^{-1}, $k_{A2} = 6.9\cdot10^5$ s^{-1}, $k_{C2} = 5.2\cdot10^5$ s^{-1}, k'' = $5.0\cdot10^6$ M^{-1} s^{-1} and k''' = $8.0\cdot10^5$ M^{-1} s^{-1} (all values except Φ_T are based on results from this work), is reported in Figure 7a. Note that P_a was the only fit variable of equation (3) to the experimental data of Figure 7a, while all the other quantities were kept fixed at the values reported above. The fit yielded $P_a = (4.6\pm0.1)\cdot10^{-7}$ Einstein L^{-1} s^{-1}, which is in very good agreement with the calculated value $P_a = \int_\lambda p°(\lambda)\,[1-10^{-\varepsilon_{AQ2S}(\lambda)\,b\,[AQ2S]}]\,d\lambda$ = $4.5\cdot10^{-7}$ Einstein L^{-1} s^{-1}.

With 3 mM AQ2S, the reaction between C and ground-state AQ2S should also be taken into account (Scheme 1c). By applying the steady-state approximation to AQ2S T_1, B, C, and $AQ2S_{red}$ one obtains the following equation:

$$R_{AQ2S} = \Phi_T P_a \cdot \frac{k_{A2}\,(k_{C2} + k'[AQ2S])}{(k_A + k''[2-\mathrm{Pr}])\,(k_C + k'[AQ2S] + k'''[2-\mathrm{Pr}])} \quad (4)$$

With the numerical values reported above and k' = $4\cdot10^9$ M^{-1} s^{-1} one can fit the experimental data of Figure 7b with equation (4). With P_a as the only fit variable, one obtains $P_a = (1.1\pm0.2)\cdot10^{-5}$ Einstein L^{-1} s^{-1}, in good agreement with the calculated value $P_a = \int_\lambda p°(\lambda)\,[1-10^{-\varepsilon_{AQ2S}(\lambda)\,b\,[AQ2S]}]\,d\lambda$ = $1.3\cdot10^{-5}$ Einstein L^{-1} s^{-1}. It should be underlined that the fit of the experimental data of Figure 7 with equations (3, 4) was carried out with P_a as the only fit variable, and P_a was also independently assessed by means of radiation absorption calculations. All the other constants were kept fixed at the values obtained in this work from laser flash photolysis measures, or from the previous fit with equation (2) of the experimental data of Figure 6. A literature value was adopted for Φ_T and kept fixed. Therefore, there is an overall consistency between laser flash photolysis data and the experimental results of Figures 6 and 7.

The agreement between the experimental data (Figures 6, 7) and the equations derived from the kinetic systems shown in Scheme 1 suggests that the water adduct C would play a key role in the photoinduced transformation of AQ2S. The latter would proceed by combination of direct photolysis and transformation sensitised by C. The direct photolysis would prevail at low AQ2S, where the main process is expected to be the transformation of C to give AQ2S hydroxyderivatives. At high AQ2S, the key process would be the reaction between C and ground-state AQ2S. The AQ2S hydroxyderivatives would be major transformation intermediates in this case as well, but a higher fraction of β-hydroxyAQ2S *vs.* α-hydroxyAQ2S would be produced compared to the former case of low AQ2S concentration.

Table 1 summarises the numerical values of the Scheme 1 kinetic parameters that were used to describe the photochemistry of AQ2S under circumneutral conditions, which are representative of most surface waters.

Table 1 Kinetic parameters (see Scheme 1) that describe the experimental data reported in Figures 6 and 7. The values of k_{A1} and k_{C1} were obtained by difference (k_A - k_{A2} and k_C – k_{C2}, respectively) as reported in the table. "LFP" = laser flash photolysis; "fit" means numerical fit of the results of steady irradiation experiments.

Kinetic parameter	Numerical value	Reference
Φ_Γ, unitless	0.18	40
k_A, s^{-1}	$(5.8\pm0.2)\cdot10^6$	This work, LFP
k_{A1}, s^{-1}	$(5.1\pm0.2)\cdot10^6$	This work, difference
k_{A2}, s^{-1}	$(6.9\pm0.1)\cdot10^5$	15 and this work, fit
k_B, s^{-1}	$(2.3\pm0.1)\cdot10^4$	This work, LFP
k_C, s^{-1}	$(3.1\pm0.1)\cdot10^6$	This work, LFP
k_{C1}, s^{-1}	$(2.6\pm0.1)\cdot10^6$	This work, difference
k_{C2}, s^{-1}	$(5.2\pm0.3)\cdot10^5$	This work, fit
k', M^{-1} s^{-1}	$(4\pm1)\cdot10^9$	16 and this work, fit
k'', M^{-1} s^{-1}	$(5.0\pm0.3)\cdot10^6$	This work, LFP
k''', M^{-1} s^{-1}	$(8.0\pm2.7)\cdot10^5$	This work, LFP

Conclusions

The triplet state AQ2S T_1 is characterised by a high spin density localised on the C=O group, which in the case of quinones is connected with significant photochemical reactivity. Such a finding supports evidence that AQ2S T_1 reacts with dissolved molecules by electron or H abstraction, which would produce a semiquinone radical.

The quantum yield of AQ2S phototransformation, Φ_{AQ2S} is independent of AQ2S up to a concentration of about 0.1 mM. Above 0.1 mM AQ2S, Φ_{AQ2S} significantly increases with increasing AQ2S concentration. The comparison and the agreement between experimental data and the results of kinetic modelling suggest that a water adduct of AQ2S, indicated here as C, would play a key role in AQ2S phototransformation. At low AQ2S, C would partly give back AQ2S and partly undergo transformation while at high AQ2S, C would mainly react with the ground-state substrate in a redox process. This reaction would cause a net AQ2S transformation and, by inhibiting the deactivation of C to AQ2S, would account for the enhancement of Φ_{AQ2S} at high substrate concentration. The proposed scenario is supported by the extent of inhibition by 2-propanol of the phototransformation of AQ2S at both low and high substrate concentration.

Fewer photoinduced processes are operational in the more dilute AQ2S solutions ([AQ2S] ≤ 0.1 mM), where Φ_{AQ2S} is also independent of [AQ2S]. Therefore, AQ2S as triplet sensitiser should be used at low concentration (≤ 0.1 mM) to avoid the additional complications that arise in more concentrated solutions, including the effect of [AQ2S] on the kinetics of AQ2S T_1 quenching.

Acknowledgements

Financial support by PNRA – Progetto Antartide and MIUR-PRIN 2009 (project n°510, area 02) is gratefully acknowledged. The work of BS in Torino was financially supported by Compagnia di San Paolo, Torino, Italy. The PhD grant of EDL was funded by Progetto Lagrange - Fondazione CRT, Torino, Italy. GM and MB thank the Auvergne region and the "Fédération des Recherches en Environnement" for the financial support. The authors also thank Blaise Pascal University for funding a one-month visit of DV in Aubiére. GM, MB and DV are grateful to Università Italo-Francese – Progetto Galileo and EGIDE for financial support of personnel exchange. AB is grateful to Prof. Eliano Diana and Prof. Carlo Nervi for precious discussion on quantum mechanical calculations. We are also grateful to anonymous reviewers for their useful suggestions.

Notes and references

[a] *Università degli Studi di Torino, Dipartimento di Chimica, Via Giuria 5, 10125 Torino, Italy. http://www.chimicadellambiente.unito.it. Fax: +39-011-6707615; Tel: +39-011-6705296; E-mail: davide.vione@unito.it*
[b] *Department of Chemical Engineering, Calcutta University, 92 Acharya P. C. Road, Kolkata 700009, India.*
[c] *Clermont Université, Université Blaise Pascal, Institut de Chimie de Clermont-Ferrand, BP 10448, F-63000, Clermont-Ferrand, France. E-mail: marcello.brigante@univ-bpclermont.fr*
[d] *CNRS, UMR 6296, ICCF,BP 80026, Aubière, France.*
[e] *Università degli Studi di Torino, Centro Interdipartimentale NatRisk, Via Leonardo da Vinci 44, 10095 Grugliasco (TO), Italy. http://www.natrisk.org*

† Electronic Supplementary Information (ESI) available: additional data of the DFT study of AQ2S T_1, LFP transient absorption spectra. See DOI: 10.1039/b000000x/

1 A. Ter Halle and C. Richard, Simulated solar light irradiation of mesotrione in natural waters, *Environ. Sci. Technol.*, 2006, **40**, 3842-3847.
2 C. K. Remucal and K. McNeill, Photosensitized amino acid degradation in the presence of riboflavin, *Environ. Sci. Technol.*, 2011, **45**, 5230-5237.
3 I. Grgic, L. I. Nieto-Gligorovski, S. Net, B. Temime-Roussel, S. Gligorovski and H. Wortham, Light induced multiphase chemistry of gas-phase ozone on aqueous pyruvic and oxalic acids, *Phys. Chem. Chem. Phys.*, 2010, **12**, 698-707.
4 J. L. Packer, J. J. Werner, D. E. Latch, K. McNeill and W. A. Arnold, Photochemical fate of pharmaceuticals in the environment: naproxen, diclofenac, clofibric acid, and ibuprofen, *Aquat. Sci.*, 2003, **65**, 342-351.
5 S. Canonica, T. Kohn, M. Mac, F. J. Real, J. Wirz and U. Von Gunten, Photosensitizer method to determine rate constants for the reaction of carbonate radical with organic compounds, *Environ. Sci. Technol.*, 2005, **39**, 9182-9188.
6 Y. Yu, M. J. Ezell, A. Zelenyuk, D. Imre, L. Alexander, J. Ortega, J. L. Thomas, K. Gogna, D. J. Tobias, B. D'Anna, C. W. Harmon, S. N. Johnson and B. J. Finlayson-Pitts, Nitrate ion photochemistry at interfaces: a new mechanism for oxidation of α-pinene, *Phys. Chem. Chem. Phys.*, 2008, **10**, 3063-3071.
7 H. Gorner, Electron transfer from aromatic amino acids to triplet quinones, *J. Photochem. Photobiol. B: Biol.*, 2007, **88**, 83-89.
8 T. Delatour, T. Douki, C. D'Ham and J. Cadet, Photosensitization of thymine nucleobase by benzophenone through energy transfer, hydrogen abstraction and one-electron oxidation, *J. Photochem. Photobiol. B: Biol.*, 1998, **44**, 191-198.
9 S. Lacombe, H. Cardy, M. Simon, A. Khoukh, J. P. Soumillion and M. Ayadim, Oxidation of sulfides and disulfides under electron transfer or singlet oxygen photosensitization using soluble or grafted sensitizers, *Photochem. Photobiol. Sci.*, 2002, **1**, 347-354.
10 J. Wenk, U. von Gunten and S. Canonica, Effect of dissolved organic matter on the transformation of contaminants induced by excited triplet states and the hydroxyl radical, *Environ. Sci. Technol.*, 2011, **45**, 1334-1340.
11 V. Maurino, A. Bedini, D. Borghesi, D. Vione and C. Minero, Phenol transformation photosensitised by quinoid compounds, *Phys. Chem. Chem. Phys.*, 2011, **13**, 11213-11221.
12 P. R. Maddigapu, C. Minero, V. Maurino, D. Vione, M. Brigante and G. Mailhot, Enhancement by anthraquinone-2-sulphonate of the

photonitration of phenol by nitrite: Implication for the photoproduction of nitrogen dioxide by coloured dissolved organic matter in surface waters, *Chemosphere*, 2010, **81**, 1401-1406.

13 P. R. Maddigapu, M. Minella, D. Vione, V. Maurino and C. Minero, Modeling phototransformation reactions in surface water bodies: 2,4-dichloro-6-nitrophenol as a case study, *Environ. Sci. Technol.*, 2011, **45**, 209-214.

14 D. Vione, P. R. Maddigapu, E. De Laurentiis, M. Minella, M. Pazzi, V. Maurino, C. Minero, S. Kouras and C. Richard, Modelling the photochemical fate of ibuprofen in surface waters, *Wat. Res.*, 2011, **45**, 6725-6736.

15 I. Loeff, A. Treinin and H. Linschitz, Photochemistry of 9,10-anthraquinone-2-sulfonate in solution. 1. Intermediates and mechanism., *J. Phys. Chem.*, 1983, **87**, 2536-2544.

16 P. R. Maddigapu. A. Bedini, C. Minero, V. Maurino, D. Vione, M. Brigante, G. Mailhot and M. Sarakha, The pH-dependent photochemistry of anthraquinone-2-sulfonate, *Photochem. Photobiol. Sci.*, 2010, **9**, 323-330.

17 H. J. Kuhn, S. E. Braslavsky and R. Schmidt, Chemical actinometry, *Pure Appl. Chem.*, 2004, **76**, 2105-2146.

18 S. E. Braslavsky, Glossary of terms used in photochemistry, *Pure Appl. Chem.*, 2007, **79**, 293-465.

19 K. P. Clark and H. I. Stonehill, Photochemistry and radiation chemistry of anthraquinone-2-sodium-sulphonate in aqueous solution. Part 1. Photochemical kinetics in aerobic solution, *J. Chem. Soc. Faraday Trans. I*, 1972, **68**, 577-590.

20 J. B. Foresman and Æ. Frisch, *Exploring chemistry with electronic structure methods*, Gaussian, Inc., Pittsburgh, PA, 1996.

21 J. A. Pople, P. M. W. Gill and B .G. Johnson, Kohn-Sham density-functional theory within a finite basis set, *Chem. Phys. Lett.*, 1992, **199**, 557-560.

22 R. G. Parr and W. Yang, *Density functional theory of atoms and molecules*, Oxford University Press, New York, 1989.

23 D. Becke, Density-functional thermochemistry. III. The role of exact exchange, *J. Chem. Phys.*, 1993, **98,** 5648-5652.

24 C. E. H. Dessent, A density functional theory study of the anthracene anion, *Chem. Phys. Lett.*, 2000, **330**, 180-187.

25 K. E. Wise, A. K. Grafton and R. A. Wheeler, Trimethyl-p-benzoquinone provides excellent structural, spectroscopic, and thermochemical models for plastoquinone-1 and its radical anion, *J. Phys. Chem. A*, 1997, **101**, 1160-1165.

26 A. K. Grafton, A. E. Boesch and R. A. Wheeler, Structures and properties of vitamin K and its radical anion predicted by a hybrid Hartree-Fock/density functional method, *J. Mol. Struct. (Theochem)*, 1997, **392**, 1-11.

27 D. Jacquemin, J. Preat, M. Charlot, V. Wathelet, J. M. Andre and E. A. Perpete, Theoretical investigation of substituted anthraquinone dyes, *J. Chem. Phys.*, 2004, **121**, 1736-1743.

28 R. Krishnan, J. S. Binkley, R. Seeger and J. A. Pople, Self consistent molecular orbital methods. XX. A basis set for correlated wave functions, *J. Chem. Phys.*, 1980, **72**, 650-654.

29 A. D. McLean and G. S. Chandler, Contracted Gaussian basis sets for molecular. calculations. I. Second row atoms, Z=11-18, *J. Chem. Phys.*, 1980, **72**, 5639-5648.

30 S. Miertus, E. Scrocco and J. Tomasi, Electrostatic interaction of a solute with a continuum: a direct utilization of ab initio molecular potentials for the prevision of solvent effects, *J. Chem. Phys.*, 1981, **55**, 117-129.

31 E. Runge and E. K. U. Gross, Density-functional theory for time-dependent systems, *Phys. Rev. Lett.*, 1984, **52**, 997-1000.

32 M. Cossi and V. Barone, Time-dependent density functional theory for molecules in liquid solutions, *J. Chem. Phys.*, 2001, **115**, 4708-4717.

33 R. W. Browne, N. M. O'Boyle, J. J. McGarvey and J. G. Vos, Elucidating excited state electronic structure and intercomponent interactions in multicomponent and supramolecular systems, *Chem. Soc. Rev.*, 2005, **34**, 641-663.

34 L. Salassa, C. Garino, G. Salassa, C. Nervi, R. Gobetto, C. Lamberti, D. Gianolio, R. Bizzarri and J. P. Sadler, Ligand-selective photodissociation from $[Ru(bpy)(4AP)_4]^{2+}$: a spectroscopic and computational study, *Inorg. Chem.*, 2009, **48**, 1469-1481.

35 M. J. Frisch, G. W. Trucks, H. B. Schlegel, G. E. Scuseria, M. A. Robb, J. R. Cheeseman, V. G. Zakrzewski, J. A. Montgomery Jr., R. E. Stratmann, J. C. Burant, S. Dapprich, J. M. Millam, A. D. Daniels, K. N. Kudin, M. C. Strain, O. Farkas, J. Tomasi, V. Barone, M. Cossi, R. Cammi, B. Mennucci, C. Pomelli, C. Adamo, S. Clifford, J. Ochterski, G. A. Petersson, P. Y. Ayala, Q. Cui, K. Morokuma, D. K. Malick, A. D. Rabuck, K. Raghavachari, J. B. Foresman, J. Cioslowski, J. V. Ortiz, B. B. Stefanov, G. Liu, A. Liashenko, P. Piskorz, I. Komaromi, R. Gomperts, R. L. Martin, D. J. Fox, T. Keith, M. A. Al-Laham, C. Y. Peng, A. Nanayakkara, C. Gonzalez, M. Challacombe, P. M. W. Gill, B. Johnson, W. Chen, M. W. Wong, J. L. Andres, M. Head-Gordon, E. S. Replogle, J. A. Pople, Gaussian 03, revision B.05, Gaussian, Inc., Pittsburgh, PA, 2003.

36 N. M. O'Boyle and J. G. Vos, GaussSum, version 1.0.5, Dublin City University, Dublin, Ireland, 2005. *http://gausssum.sourceforge.net*, last accessed September 2011.

37 R. S. K. A. Gamage, B. M. Peake and J. Simpson, X-Ray crystal structure determination of some sodium anthraquinone sulfonate derivatives, *Aust. J. Chem.*, 1993, **46**, 1595-1604.

38 V. Maurino, D. Borghesi, D. Vione and C. Minero, Transformation of phenolic compounds upon UVA irradiation of anthraquinone-2-sulfonate, *Photochem. Photobiol. Sci.*, 2008, **7**, 321-327.

39 B. Sui and X. Fu, Novel application of 1-/2-phenyl substituted 9,10-anthraquinones in solid electrochromic devices, *J. Solid State Electrochem.*, 2009, **13**, 1889-1895.

40 A. E. Alegría, A. Ferrer,. G. Santiago, E. Sepúlveda and W. Flores, Photochemistry of water-soluble quinones. Production of hydroxyl radical, singlet oxygen and the superoxide ion, *J. Photochem. Photobiol. A: Chem.*, 1999, **127**, 57-65.

41 J. N. Moore, D. Phillips and R. E. Hester, Time-resolved resonance Raman spectroscopy applied to the photochemistry of the sulfonated derivatives of 9,10-anthraquinone, *J. Phys. Chem.*, 1988, **92**, 5619-5627.

42 I. Loeff, S. Goldstein, A. Treinin and H. Linschitz, Interactions of formate ion with triplets of anthraquinone-2-sulfonate, 1,4-naphthoquinone, benzophenone-4-carboxylate, and benzophenone-4-sulfonate, *J. Phys. Chem.*, 1991, **95**, 4423-4430.

43 B. E. Hulme, E. J. Land and G. O. Phillip, Pulse radiolysis of 9,10-anthraquinones. Part 1. Radicals, *J. Chem. Soc. Faraday Trans. I*, 1972, **68**, 1992-2002.

44 J. N. Moore, D. Phillips, N. Nakashima and K. Yoshihara, Photochemistry of 9,10-anthraquinone-2,6-disulphonate, *J. Chem. Soc. Faraday Trans. 2*, 1986, **82**, 745-761.

45 D. Phillips, J. N. Moore and R. E. Hester, Time-resolved resonance Raman spectroscopy applied to anthraquinone photochemistry, *J. Chem. Soc. Faraday Trans. 2*, 1986, **82**, 2093-2104.

46 B. Sur, M. Rolle, C. Minero, V. Maurino, D. Vione, M. Brigante and G. Mailhot, Formation of hydroxyl radicals by irradiated 1-nitronaphthalene (1NN): oxidation of hydroxyl ions and water by the 1NN triplet state, *Photochem. Photobiol. Sci.*, 2011, **10**, 1817-1824.

47 R. S. Silva and D. E. Nicodem, Deuterium isotope effects on the photoreduction of 9,10-phenanthrenequinone and benzophenone by 2-propanol. *J. Photochem. Photobiol. A: Chem.*, 2008, **194**, 76-80.

48 H. Nagakubo, G. Kubota, K. Kubo, T. Kaneko, T. Sakurai and H. Inoue, Self-sensitized photolysis of N-(1-naphthoyl)-N-phenyl-O-(benzoyl-substituted benzoyl)hydroxylamines, *Bull. Chem. Soc. Japan*, 1996, **69**, 2603-2611.